Actinyl Ions in $Cs_2UO_2Cl_4$

Spiridoula Matsika and Russell M. Pitzer*

Department of Chemistry, The Ohio State University, 100 West 18th Avenue, Columbus, Ohio 43210

Received: August 23, 2000; In Final Form: October 17, 2000

The electronic energy levels of the uranyl ion (UO_2^{2+}) and the neptunyl ion (NpO_2^{2+}) in the crystalline environment of $Cs_2UO_2Cl_4$ are studied theoretically and compared with the spectroscopic work of Denning and co-workers. A layered-cluster computational method is used. The valence electrons of the actinyl ion and the nearest-neighbor chloride ions are treated explicitly, the closest cesium ions are replaced by all-electron core potentials, and all ions further away are replaced by point charges. The cluster is approximately spherical overall and contains 1873 ions. For the electrons treated explicitly, we use relativistic quantum chemical theory, including relativistic effective core potentials, corresponding spin−orbit operators, and spin−orbit, graphical unitary group configuration interaction. The effects of the crystalline environment on bond distances, vibrational frequencies, excitation energies, energy splittings, and wave function character are examined. Shifts are generally more accurate than absolute values, and the electron correlation treatment is generally the limiting factor in the accuracy.

1. Introduction

Actinyl ions are important for the understanding and treatment of nuclear waste.[1−3] Most actinides in their high oxidation states exist as actinyl ions. Theoretical methods for investigating the properties of actinides are advantageous in that it is not necessary to deal with radioactive material, but they have some disadvantages as well, one of which is the fact that, due to computational limitations, large systems are difficult to calculate. As a consequence, in the case of actinyl ions, most existing calculations are for the free ions. Actinyl ions, however, hardly ever exist in the gas phase; they are either in solutions or in crystals. Only uranyl has been synthesized in the gas phase (in thermochemical characterization experiments[4]). Thus it would be useful if theoretical models could incorporate the effects of the crystal or solution environments.

Computational chemistry has advanced considerably in gas-phase studies, where a molecular system can be considered as an isolated species. This is not true, however, for condensed phases, where the molecule exists in contact with other molecules. Several groups have realized the importance of introducing the condensed-phase environment in calculations. A variety of models exist for incorporating the effects of the solvent. One widely used approach is to treat the solvent as a dielectric continuum.[5] Other approaches retain the molecular (microscopic) level of description.[6]

For calculations of crystal systems there are two common approaches.[7,8] The first approach uses the periodicity of the crystal and Bloch's theorem for translational symmetry. The orbitals obtained from such methods are delocalized and are best suited for perfect crystals. The second approach follows the philosophy that when the properties of interest in the system are localized within a small region, one can concentrate one's efforts in this region and use approximations for the remainder of the crystal. The simplest approach is to consider only the nearest neighbors and disregard the rest of the crystal. This approach was used by Sugano and Shulman[9] in the first application of a cluster approximation to a crystal. The next step in ionic crystals involves taking into account the Madelung potential of the surrounding crystal; this can be done by putting point charges around the cluster to represent the crystal lattice[10−13] or by calculating the external lattice potential using the Ewald method[14] and representing it analytically.[15−17] This takes care of the electrostatic interactions between the cluster and the lattice but does not account for any short-range quantum interactions. Pseudopotentials[18−21] or model potentials[22] have been developed and used which can represent short-range interactions without increasing the computational cost dramatically. Lattice-relaxation and polarization can also be taken into account.[23] More sophisticated methods treat the whole crystal even more accurately.[24−31]

In the present work we try to incorporate the crystal environment effects for two of the actinyl ions, uranyl and neptunyl. Uranium is the last element in the periodic table observed extensively in nature and is the raw material from which the subsequent man-made actinides are synthesized. Uranyl, the most well-known actinyl ion, has been studied since 1789[32] and was involved in the coining of the word fluorescence and the formulation of Stokes Law[33] and the discovery of radioactivity.[34] The green fluorescence of the first excited state is the most characteristic optical feature of uranyl. Many papers have been published reporting spectra,[33,35−42] trying to interpret the spectra,[43−47] or calculating the electronic structure of uranyl.[4,48−73] The importance and extent of the work done on uranium and uranyl compounds can be measured by the number of books[36,38,74] and reviews[75,76] written on the subject. Some of the most debated matters about the electronic structure of uranyl have been the ordering of the molecular orbitals (MO's), the nature of the excited states, and the nature of the bonding. It took many years, but the basic characteristics of the electronic spectrum of uranyl are now understood.

Neptunium is next to uranium in the periodic table and is the first man-made actinide. Studies on the neptunyl ion are limited compared to those on the uranyl ion. Its electronic spectrum has been reported and studied.[77−85] Theoretical

* Corresponding author. E-mail address: pitzer.3@osu.edu.

10.1021/jp003032h CCC: $20.00
Published on Web 12/13/2000

calculations[61,86−90] have added to the understanding of the features of the spectrum. Several of the questions regarding neptunyl are related to those of uranyl.

The electronic spectroscopy for both uranyl and neptunyl ions was clarified by the detailed work of Denning et al.,[39−42,47,76,83,84] in $Cs_2UO_2Cl_4$ and $CsUO_2(NO_3)_3$ crystals. Absorption spectroscopy in these particular crystals had been observed prior to Denning, but not in sufficient detail to make firm assignments of the observed lines.[36,81,82] Denning and co-workers reported polarized, single-crystal absorption spectra of $Cs_2UO_2Cl_4$ and $Cs_2U(Np)O_2Cl_4$ at 4.2 K. They were able to assign 12 excited states for uranyl and 10 for neptunyl. Later they reported two-photon spectra for $Cs_2UO_2Cl_4$, which helped them to identify one more state in uranyl.[42] They used an extensive series of arguments, based mainly on their high-resolution spectra, to assign the uranyl spectrum.

The highest closed-shell MO's in uranyl, and in actinyl ions in general, are σ_g, π_g, σ_u, and π_u, which are composed of O 2p orbitals with some mixing of An 5f and 6d orbitals. These MO's are close in energy and it is difficult to determine from theoretical or experimental results which MO is the HOMO. The fundamental question, however, is slightly different and is from which of these MO's the excitations occur in uranyl. Previously there had been arguments supporting each one of these MO's. Jørgensen[46] argued that the low intensity of the observed transitions was due to the parity selection rule; the spin−orbit coupling is sufficiently large in actinides that the spin selection rule seemed unlikely to be able to cause the observed low intensities. The orbitals to which the electron is excited are f (ungerade), so the excitation should occur from an ungerade orbital. This argument reduces the possibilities to half, only the σ_u and π_u orbitals being eligible. Görller-Walrand and Vanquickenborne[44] used the crystal field splittings of the uranyl excited states due to equatorial ligands to decide on the possible coupling and nature of states involved. Their analysis showed that $\Lambda-S$ is the most appropriate coupling scheme and that the orbital from which excitation occurs is a σ_u orbital. Denning et al. confirmed this by pointing out that twice as many excited states result from a π_u excitation as from a σ_u excitation, contrary to their observations. They used the magnetic moment of the fluorescent state to assign it. This moment was measured to be very close to zero, which can only occur if the spatial contribution cancels the spin contribution. For two unpaired electrons this can only occur in a $^3\Delta_1$ state, which in this case must correspond to the configuration $\sigma_u\delta_u$, giving a $^3\Delta_{1g}$ state.

Some calculations have been reported with equatorial ligands around the uranyl[50,56,59−63,66−68,72,73] or neptunyl[61,62,68,89] ion. The ligands varied from fluorides and chlorides to nitrates, sulfates, carbonates, hydroxides, water molecules, and even just point charges. A variety of methods was used, with density functional theory being the most sophisticated way of including correlation and four-component methods being the most sophisticated way of including the relativistic effects. Most of these calculations were primarily concerned with the effect of the ligands on the bonding and the geometry of the actinyl ions. Interestingly, Schreckenbach et al.[66] found local minima for $UO_2(OH)_4^{2-}$ with a bent uranyl unit only 18−19 kcal/mol higher in energy than the global minimum. Makhyoun[89] calculated f → f transitions for $NpO_2Cl_4^{2-}$ and $NpO_2(NO_3)_3^-$ using the X_α and Slater transition-state procedures.[91]

We model the $Cs_2UO_2Cl_4$ crystal in trying to answer questions concerning the influence of the crystal environment on the spectroscopy[76] of actinyl ions. The uranyl spectroscopy was done in the pure $Cs_2UO_2Cl_4$ crystal, while the neptunyl spectroscopy was done by doping this crystal with a small amount of neptunium, $Cs_2U(Np)O_2Cl_4$.

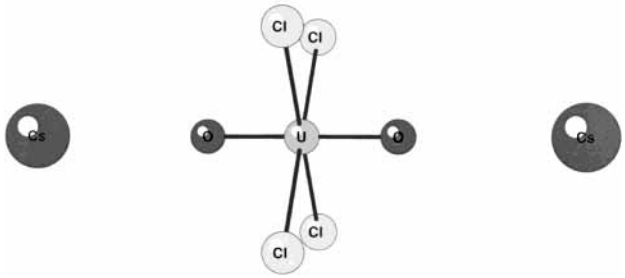

Figure 1. $Cs_2UO_2Cl_4$ local structure.

The X-ray crystallography of $Cs_2UO_2Cl_4$ was first done by Hall et al.[92] in 1966 and, 25 years later, more accurately, by Watkin et al.[93] It has a monoclinic structure, C2/*m* space group, and unit cell dimensions $a = 11.929(2)$, $b = 7.704(2)$, $c = 5.816(2)$ Å, and $\beta = 100.02(4)°$. The uranyl ion is linear, as expected, with a U−O distance of 1.774(4) Å; four chlorides are in a plane perpendicular to the O−U−O axis. The Cl−U−Cl angle is very close to a right angle, 92.9°. The site symmetry of uranium is C_{2h}, close to D_{2h} and moderately close to D_{4h}. The local structure of $Cs_2UO_2Cl_4$ is shown in Figure 1. $Cs_2UO_2Cl_4$ crystals dilute in Np are isostructural to the pure $Cs_2UO_2Cl_4$ crystal.[83] This facilitates our calculations, since we only need to model one crystal and then substitute the central atom as either U or Np to study the uranyl or neptunyl ion, respectively.

2. Methods

2.1. Crystal Model. The model of the crystal in this work follows the work of Winter et al.[18−21] The crystal model is divided into three layers. The emphasis is on the actinyl ions, so the central actinyl ion and the four chlorides that surround it are treated with standard ab initio methods, as described in the next subsection. In this way both the ligand field and crystal field effects are incorporated into the calculations. The next nearest neighbors are six cesium ions. These are described by all-electron potentials.[94] Subsequent shells are described by point charges; for every such UO_2^{2+} unit a +2 point charge is positioned at the experimental position of U, for every Cl^- a −1 point charge is used, and for every Cs^+ a +1 point charge is used. The need to have an intermediate shell between the ab initio cluster and the point-charge lattice has been investigated in detail.[19−21] If only point charges are used for the lattice, the interaction between atoms in the two layers is not adequately described. Point charges describe the Coulomb attraction or repulsion, but the short-range interaction within the range of the atomic orbitals of the ab initio cluster must be described also. It was found[21] that the problem is the most serious in the interaction between oppositely charged ions. All-electron potentials can describe these short-range interactions adequately.

Point charges were added to the lattice, retaining its symmetry, until the Madelung (Ewald) potential in the region of the central atoms converged. Properties of interest were also calculated to make sure that they converged. These were the An−O distance in the central actinyl ion, the O−An−O symmetric-stretch vibrational frequency, and some transition energies. Another requirement when deciding where to terminate the lattice was to try and make the total charge as close to zero as possible. The lattice chosen has 1873 ions extending to a distance of 25 Å; it is shown in Figure 2.

2.2. Ab Initio Methods. Relativistic effective core potentials[95] are used to reduce the number of electrons requiring explicit

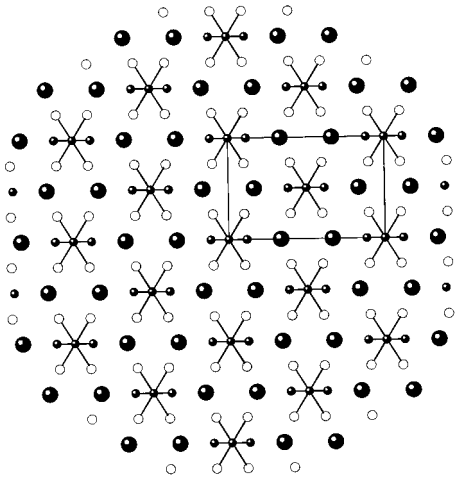

Figure 2. *c*-Axis projection of the structure of $Cs_2UO_2Cl_4$.

treatment and to take account of the large relativistic effects in the core region. The actinide (U or Np) core consists of the 78 1s through 5d electrons, the O core consists of the 2 1s electrons, and the Cl core consists of the 10 $1s^22s^22p^6$ electrons.

The basis sets are contracted Gaussian basis sets which have been developed in our group[96] following the correlation-consistent method of Dunning.[97] All are of approximately polarized double-ζ size: U (4sd4p4f1g)/[3sd2p2f1g], O (4s4p1d)/[2s2p1d], Cl (4s4p1d)/[2s2p1d].

The MO's for use in subsequent configuration interaction (CI) calculations were generated from average-of-states self-consistent-field (SCF) or multiconfiguration-SCF (MCSCF) calculations. It is well-known that actinide atoms in actinyl ions interact more weakly with the equatorial ligands than with the (axial) oxygen atoms, so the electronic structure of these ions is primarily determined by the axial interactions. Thus in the present crystal studies we use the information previously obtained for the free actinyl ions.[71,90]

The ground state of uranyl has a closed-shell electron configuration, $1\sigma_g^2 2\sigma_g^2 1\sigma_u^2 2\sigma_u^2 1\pi_u^4 1\pi_g^4 2\pi_u^4 3\sigma_g^2 3\sigma_u^2$ (only the U 6s6p5f6d7s and the O 2s2p electrons participate in this configuration since the others are in the core). The lowest excited states involve excitations from the $3\sigma_u$ doubly occupied MO to the unoccupied U f orbitals. In linear symmetry the f orbitals split into σ_u, π_u, δ_u, and ϕ_u orbitals. The $5f\delta_u$ and $5f\phi_u$ orbitals are nonbonding and lower in energy, so the lowest excited states will involve excitations to these orbitals. This is true in the free uranyl ion and has been established both experimentally and theoretically.[71,76] In the crystal these states continue to be the lowest energy excited states and are the ones included in our calculations. In the free uranyl ion calculations it was found that excitations from $2\pi_u$ to $3\pi_u$ had large single-excitation coefficients in the CI expansion;[71] this is an indication that the $2\pi_u$ MO's are not optimum for correlation. The way to improve these orbitals is to do a $(2\pi_u,3\pi_u)$ rotation. This can be done by a complete-active-space (CAS) MCSCF calculation in the $(2\pi_u,3\pi_u)$ space. In the crystal calculations we followed this procedure, so the MO's were taken from average-of-states MCSCF calculations. The states included in the average were the ground state and the lowest excited states, the latter arising from the configurations $3\sigma_u^1 1\delta_u^1$ and $3\sigma_u^1 1\phi_u^1$. The natural orbitals were used.

The ground state in neptunyl is formed from a mixture of δ_u^1 and ϕ_u^1 configurations. The excited states arise either from excitations to another f orbital or, as in uranyl, excitation from $3\sigma_u$ to one of the f orbitals. The states averaged at the SCF level to obtain the MO's were the $^2\Delta_u$ (δ_u^1), $^2\Phi_u$ (ϕ_u^1), ^4H_u ($3\sigma_u^1\delta_u^1\phi_u^1$), and $^4\Pi_u$ ($3\sigma_u^1\delta_u^1\phi_u^1$). In this case the phenomenon observed in uranyl, of large $2\pi_u \rightarrow 3\pi_u$ single-excitation coefficients caused by nonoptimum orbitals, was not observed.

TABLE 1: Resolution of the Symmetry Species of the $D_{\infty h}$ Point Group into Those of the D_{4h} and the C_{2h} Point Groups

$D_{\infty h}$	D_{4h}	C_{2h}
σ_g	a_{1g}	a_g
π_g	e_g	$a_g + b_g$
σ_u	a_{2u}	b_u
π_u	e_u	$a_u + b_u$
δ_u	$b_{1u} + b_{2u}$	$a_u + b_u$
ϕ_u	e_u	$a_u + b_u$

In the previous two paragraphs, linear symmetry notation was used to make apparent the connection between linear symmetry and the crystal symmetry. In the crystal structure the site symmetry of the actinides is C_{2h}; in this lowered symmetry the orbitals split. Table 1 shows how the linear symmetry orbitals transform in D_{4h} and C_{2h} symmetries. In the following discussion we will be using both $D_{\infty h}$ and C_{2h} notation, as appropriate.

Multireference spin−orbit singles-and-doubles CI calculations were performed using the spin−orbit CI program based on the graphical unitary group approach (GUGA) formalism.[98] The references for uranyl were the ground state and the $3\sigma_u^1 1\delta_u^1$ and $3\sigma_u^1 1\phi_u^1$ configurations. The references for neptunyl were the $3\sigma_u^2 1\delta_u^1$, $3\sigma_u^2 1\phi_u^1$, $3\sigma_u^2 3\pi_u^1$, $3\sigma_u^1 1\delta_u^1 1\phi_u^1$, $3\sigma_u^1 1\delta_u^2$, and $3\sigma_u^1 1\phi_u^2$ configurations.

In all calculations all the occupied chlorine MO's were frozen. In the uranyl calculations the $1\sigma_g$, $2\sigma_g$, $1\sigma_u$, and $1\pi_g$ MO's were also frozen. There were 5 305 686 double group functions (dgf) in the CI expansion. Neptunyl has one more electron and many more references, which increase the computational cost substantially, so the $2\sigma_u$, $1\pi_u$, and $3\sigma_g$ MO's were also frozen. In addition, two calculations had to be performed, the first with the f-type references and the second with the charge-transfer type references. The resulting sizes of the CI expansion were 1 649 686 dgf in the first case and 4 665 786 dgf in the second case. The adiabatic transition energies were calculated for 17 states of uranyl and 12 states of neptunyl.

Additional calculations with more correlation were carried out for the ground state of the neptunyl ion. These calculations have the same number of frozen orbitals as the uranyl ones. They were performed so that a more direct comparison can be done between the two ions. Although such large calculations were not possible for the excited states of neptunyl, they were possible for the ground state because the reference space is much smaller. The number of dgf for these calculations was 6 661 284.

The symmetric-stretch vibrational frequencies reported here were calculated by fitting the potential energy surface along the An−O coordinate to a quadratic polynomial. Thus, anharmonicity was neglected. The potential energy surfaces were generated by single point calculations where the An−O distance was symmetrically stretched or contracted by 0.01 Å. There are three modes of vibration in triatomic actinyl ions. The symmetric-stretch vibrational frequency is given by $\nu_1 = (f/m_O)^{1/2}$, where the force constant f is equal to the quadratic coefficient of our quadratic polynomial. The quality of the frequencies calculated depends not only on the quality of the ab initio methods for calculating the potential surface but also on the fitting and the validity of the harmonic approximation. Therefore the quality of the calculated frequencies is less than that of the calculated bond distances.

TABLE 2: Ground-State Tetrachlorouranyl SCF Mulliken Population Analysis

	gross atomic populations					
atom	s	p	d	f	g	total
U	2.195	5.667	1.718	2.339	0.003	11.922
O	3.851	9.131	0.042			13.023
Cl	7.913	23.119	0.022			31.054

TABLE 3: U−O Bond Distance and Symmetric-Stretch Vibrational Frequency for the Ground State of the Uranyl Ion as a Free Ion and in the $Cs_2UO_2Cl_4$ Crystal

system (method)	R_e (Å)	ν_1, cm^{-1}
free ion (SCF)	1.65	1156
free ion (CI)	1.67	1104
free ion (DHF + CCSD(T))[a]	1.715	974
crystal (SCF)	1.72	932
crystal (CI)	1.73	968
crystal (experiment)	1.774[b]	832[c]

[a] From de Jong et al.[65] [b] From Watkin et al.[93] [c] From Denning et al.[40]

3. Results and Discussion

3.1. UO_2^{2+}. As discussed earlier, the ground state of uranyl is a closed shell, 0^+_g in linear symmetry and A_g in double group C_{2h} symmetry. It is nondegenerate, so no interaction can split it.

The Mulliken population analysis for UO_2^{2+} in the crystal is shown in Table 2 at the distance R_e(U−O) = 1.73 Å. The charge on U is +2.078 as opposed to +2.423 for the free uranyl ion[71] at its calculated minimum. The charge on each O is −0.511, while for the free ion it is −0.211. Each of the four chlorides has a −0.763 charge. The additional electronegative ligands have decreased the uranium positive charge by a small amount. It is evident that although the extreme ionic model is useful in assigning oxidation states and explaining the electronic structure in these ions, this model is far from reality. Another common feature in the early actinyl ions is the 6p hole, which appears in the crystal also; the U 6p population is 5.7 instead of 6.

DeKock et al.[56] in their $UO_2F_4^{2-}$ calculations argue that the $3\sigma_u$ orbital, from which excitations occur, has a reduced uranium character in the complex and about 65% fluorine character. Denning and co-workers[42] find no evidence for this in their spectrum on the analogous $UO_2Cl_4^{2-}$; if this mixing occurred the U−Cl stretch would change significantly from the ground to the excited states and would affect the vibrational progressions for this mode. In their spectrum the U−Cl vibrational frequencies are almost identical in the ground and excited states; what changes significantly are the U−O modes. Our calculations agree with Denning's conclusion; the $3\sigma_u$ orbital does not have much chlorine mixing. Even more, none of the other uranyl orbitals mix significantly with the chlorine orbitals.

Table 3 compares the ground-state U−O bond distance and symmetric-stretch vibrational frequency for the uranyl ion in the crystal with that of the free uranyl ion at the SCF and CI levels of theory. The effect of the ligands surrounding UO_2^{2+} in the crystal is to stretch the oxygen atoms further away from the central U atom and to weaken the bonds. This is shown by the results in Table 3; R_e(U−O) increases by 0.07 Å in the crystal and ν_1 decreases by 224 cm^{-1} at the SCF level. At the CI level the differences are 0.06 Å and 136 cm^{-1}, respectively. The comparison at the CI level, however, is not as simple. The calculations for the crystal involve more electrons and more basis functions, which results in much larger CI expansions. To be able to do these calculations we had to reduce the number of electrons correlated, as was explained in the methodology section. The CI calculations for the free ion had all 25 electrons correlated, but the CI calculations in the crystal had only 15 electrons correlated. This difference in correlation complicates direct comparisons of the results. The experimental R_e and ν_1 are also shown here from the work of Denning and co-workers.[40,93] The largest difference between the free-ion calculations and the experimental results is due to the different environment.

TABLE 4: U−O Bond Distances (in Å) of the Excited States of UO_2^{2+} in $Cs_2UO_2Cl_4$

C_{2h}	$Cs_2UO_2Cl_4$	UO_2^{2+} [a]	$D_{\infty h}$
A_g	1.728	1.668	0^+_g
B_g	1.790	1.733	1_g
A_g	1.789		
B_g	1.792	1.739	2_g
A_g	1.790		
A_g	1.794	1.742	3_g
B_g	1.794		
A_g	1.806	1.749	2_g
B_g	1.806		
A_g	1.804	1.747	3_g
B_g	1.805		
A_g	1.807	1.755	4_g
B_g	1.808		
B_g	1.816		3_g
A_g	1.816		
A_g	1.816		2_g
B_g	1.817		

[a] From Zhang and Pitzer.[71]

But there is still a discrepancy due to the limitation of our methods. Table 3 includes another theoretical calculation for the free uranyl ion. These results are from four-component Dirac calculations (DHF) using the coupled-cluster method (CCSD(T)) for correlation.[65] These methods are more accurate than the present work and their results are among the most accurate results reported for uranyl. The difference between their bond distance and the experimental one (0.06 Å) is equal to the difference between our calculated distances in the free-ion and crystal calculations. This is almost true for the same comparison using frequencies instead of distances (142 vs 136 cm^{-1}). This suggests that the DHF + CCSD(T) results are very close to the true values for the gas-phase uranyl ion and that our calculated effects of the crystal on the values of R_e and ν_1 are accurate.

The lowest excited states in uranyl arise from excitation from the $3\sigma_u$ orbital to the $1\delta_u$ or $1\phi_u$ orbitals. The corresponding configurations are $3\sigma_u^1 1\delta_u^1$, $3\sigma_u^1 1\phi_u^1$, and the states in $\Lambda-S$ notation are $^3\Delta_g$, $^1\Delta_g$, $^3\Phi_g$, $^1\Phi_g$. When spin−orbit coupling is introduced, $^3\Delta_g$ gives $\Omega = 1, 2, 3$, $^1\Delta_g$ gives $\Omega = 2$, $^3\Phi_g$ gives $\Omega = 2, 3, 4$, and $^1\Phi_g$ gives $\Omega = 3$. The states with the same Ω value mix, and this makes a multireference CI calculation a necessity. The crystal field, when uranyl is in the crystal, will split all these excited states into two components. The equilibrium U−O bond distances and symmetric-stretch vibrational frequencies have been calculated for the 16 excited states and compared with the free-ion calculations. Table 4 compares the equilibrium U−O bond distances between the crystal and the free ion. The Ω values ($D_{\infty h}$ double group symmetry) and the C_{2h} double group symmetry for each state are in columns 4 and 1, respectively. Similarly, Table 5 compares the calculated symmetric-stretch vibrational frequencies for these states with the calculated free-ion frequencies[71] and the experimental frequencies measured by Denning et al.[40] from the progressions in the electronic spectrum. As for the ground state, the U−O bonds are weaker in the crystal for all of these states. All the excited states of uranyl involve an excitation from a bonding

TABLE 5: Symmetric-Stretch Vibrational Frequencies (in cm^{-1}) of the Excited States of UO_2^{2+} in $Cs_2UO_2Cl_4$

C_{2h}	calcd $Cs_2UO_2Cl_4$	exptl $Cs_2UO_2Cl_4$[a]	calcd UO_2^{2+}	$D_{\infty h}$
A_g	968	832	1103	0_g^+
B_g	885	714.8	867	1_g
A_g	885	714.6		
B_g	879	710.3	845	2_g
A_g	878	696		
A_g	874	712	847	3_g
B_g	874	710		
A_g	902	717	900	2_g
B_g	900	711		
A_g	903	724.7	898	3_g
B_g	904	724.3		
A_g	890	705.4	880	4_g
B_g	896	708		
B_g	890			3_g
A_g	890			
A_g	873	680 ± 3		2_g
B_g	872	734 ± 5		

[a] From Barker et al.[42] [b] From Zhang and Pitzer.[71]

TABLE 6: Character and Excitation Energies of the Excited States of UO_2^{2+} in $Cs_2UO_2Cl_4$

state	$\Lambda-S$ term	T_e, cm^{-1}	T_e, cm^{-1} (exptl)[a]
A_g	89% $^1\Sigma^+$	0	0
A_g	89% $^3\Delta$	20 364	20 095.7
B_g	89% $^3\Delta$	20 363	20 097.3
B_g	79% $^3\Delta$ + 10% $^3\Phi$	21 013	20 406.5
A_g	78% $^3\Delta$ + 11% $^3\Phi$	21 838	21 316
A_g	70% $^3\Delta$ + 15% $^3\Phi$	22 808	22 026.1
B_g	71% $^3\Delta$ + 14% $^3\Phi$	22 830	22 076
A_g	9% $^3\Delta$ + 74% $^3\Phi$	24 618	22 406
B_g	8% $^3\Delta$ + 76% $^3\Phi$	24 780	22 750
A_g	19% $^3\Delta$ + 62% $^3\Phi$	26 763	26 197.3
B_g	19% $^3\Delta$ + 61% $^3\Phi$	26 871	26 247.6
B_g	89% $^3\Phi$	29 169	27 719.6
A_g	89% $^3\Phi$	29 145	27 757
B_g	75% $^1\Phi$ + 14% $^3\Phi$	31 940	
A_g	76% $^1\Phi$ + 12% $^3\Phi$	32 063	
A_g	81% $^1\Delta$ + 4% $^3\Phi$	33 510	29 277
B_g	83% $^1\Delta$ + 3% $^3\Phi$	34 159	29 546

[a] From Denning.[76]

orbital ($3\sigma_u$) to a nonbonding orbital. When such an excitation occurs the bond weakens and the excited-state potential curves move to larger distances and are more flat. This is shown in Table 4.

As was said earlier, states with the same Ω and parity values can mix substantially. Here these states are $^3\Delta_{2g}$ with $^3\Phi_{2g}$ and $^3\Delta_{3g}$ with $^3\Phi_{3g}$. Table 6 shows that this occurs for uranyl in the crystal also. The basic characteristics of these electronic states do not change much in the crystal environment. The first 12 excited states are triplets and the next four are singlets. This demonstrates that even in these ions where the spin−orbit coupling constants are large (ca. 2000 cm^{-1}), $\Lambda-S$ coupling is a useful approximation and Hund's first rule is still applicable.

The adiabatic excitation energies for the 16 calculated excited states are also shown in Table 6. These are compared with the experimental excitation energies from Denning.[76] The first calculated excited state with mostly singlet character (14th and 15th states in Table 6) has mostly Φ character and corresponds to $\Omega = 3$ in linear symmetry. In Denning's work, though, a state with mostly Δ character and $\Omega = 2$ was found. The free-ion calculations agree with our calculations in this ordering. The average difference between our calculated energies and the experimental energies is 1450 cm^{-1}. If the last states, where the ordering between experiment and theory is different, are omitted, the average difference drops to 955 cm^{-1}.

TABLE 7: Comparison of Excitation Energies (in cm^{-1}) of UO_2^{2+}

state	$Cs_2UO_2Cl_4$	$Cs_2UO_2Cl_4$[a]	$CsUO_2(NO_3)_3$[b]	UO_2^{2+} [c]	UO_2^{2+} [d]
0_g^+	0	0	0	0	0
1_g	20 363	20 096	21 090	20 366	20 719
2_g	21 425	20 861	21 694	20 930	21 421
3_g	22 819	22 051	22 786	22 105	22 628
2_g	24 699	22 578	23 474	23 154	23 902
3_g	26 817	26 222	27 062	25 448	26 118
4_g	29 157	27 738	29 618	27 196	27 983
3_g	32 001			30 573	31 710
2_g	33 834	29 412	31 262	34 705	

[a] From Denning,[76] with splittings averaged out. [b] From Denning et al.,[41] with splittings averaged out. [c] 14 electrons correlated. [d] From Zhang and Pitzer.[71]

TABLE 8: Vertical SCF Transition Energies (in cm^{-1}) of Uranyl in the Crystal and as a Free Ion

C_{2h}	$Cs_2UO_2Cl_4$	UO_2^{2+}	$D_{\infty h}$
^1A_g	0	0	$^1\Sigma_g$
^3A_g	21 524	23 691	$^3\Delta_g$
^3B_g	22 309		
^3B_g	28 806	29 121	$^3\Phi_g$
^3A_g	28 988		

Table 7 compares the calculated and experimental crystal excitations, with their crystal-field splittings averaged out, to free-ion calculations. All the calculated transitions are adiabatic. The left column has the Ω value for each state in linear symmetry, the second column has the calculated transitions for the crystal, the third and fourth columns have experimental transitions for $Cs_2UO_2Cl_4$ and $CsUO_2(NO_3)_3$ respectively, and columns five and six have free-ion calculated transitions. The transitions in column six are from previous work.[71] In these calculations the MO's were obtained in the same way, the same references were included in the CI, and all electrons were correlated. Thus, these calculations are similar to the ones in the crystal except for the number of correlated electrons. To eliminate this difference we performed some calculations for the free uranyl ion where the same electrons as in the crystal were correlated. A difference that cannot be eliminated is that in the crystal calculations there are virtual orbitals from the chlorides. Although all occupied chloride orbitals were frozen in the crystal, the virtuals were not, since they mix with the other orbitals and they cannot be separated in a straightforward way. The results from these calculations are shown in column five and these are the results we will use to compare with the crystal calculations. By looking at this table we see that the shifts of the transitions due to the crystal environment are not very large, ranging from 3 to 2000 cm^{-1}. This is also true when comparing the two experimental transitions for different crystals. Transitions to the first and eighth excited states are red-shifted, while transitions to all the other states are blue-shifted. What is common between the two red-shifted states is that they are pure Δ without any Φ mixing.

Differences between the free-ion and crystal calculations caused by correlation and spin−orbit effects can be eliminated by comparing the SCF transition energies. The SCF transition energies are not to be taken seriously as absolute numbers; the only purpose of calculating at this level is to make additional comparisons. As can be seen in Table 8 the excitations are red-shifted for both the $^3\Delta_g$ and $^3\Phi_g$ states. The shift for the $^3\Delta_g$ state, however, is much larger, as is the splitting. From both the SCF and CI results it seems that Δ states stabilize in the crystal more than Φ states. This effect is even more pronounced in neptunyl and will be discussed extensively in that section.

TABLE 9: Crystal-Field Splittings (in cm^{-1}) of the Excited States of Uranyl

state	calcd splitting	exptl splitting[a]
0_g^+	0	0
1_g	−1	1.6
2_g	825	910
3_g	22	50
2_g	162	344
3_g	108	50
4_g	−24	37
3_g	123	
2_g	649	269

[a] From Denning.[76]

Denning's review[76] contains a correlation graph between the first uranyl excited-state energy and the U−O bond length for different compounds. His observation is that weaker bonds (longer bond length) raise the energy of the σ_u orbital and thus decrease the energy of the first excited state. The more negative or basic the equatorial ligands, the more they weaken the bond. Following this argument, the transition to the first excited state in the crystal should be at lower energies than that of the free ion, and this is true in our calculations. It is also true for all excited states at the SCF level but not at the CI level. This could be because more complicated effects drive this behavior or because our calculations fail to compute all states equivalently.

One effect that the crystal environment has on the electronic states is to shift the transitions; another one is that it splits the excited states, so the electronic spectrum has double peaks instead of single peaks. The crystal field splitting for the excited states of uranyl is shown in Table 9. Theoretical calculations can predict this splitting much better than the absolute transition energies, since the crystal field is a one-electron operator to a good approximation. Another important point is that the magnitude of these splittings differs from state to state. Görller-Walrand and Vanquickenborne[44] analyzed the splittings of these states; in the crystal field of the ligands, V_{CF}, the energy splitting is given by matrix elements

$$\Delta E = \langle \Psi(\Omega) | V_{CF} | \Psi(-\Omega) \rangle$$

where $\Psi(\Omega)$ is the wave function of a state Ω. Since V_{CF} can be approximated as a sum of one-electron operators, the splitting will be zero to first order in perturbation theory unless $\Psi(\Omega)$ and $\Psi(-\Omega)$ differ by only one spin−orbital. This is true for two-electron wave functions only if the coupling is $\Lambda-S$, if one of the orbitals is a σ orbital, and if the projection of total spin, $\sum$, is zero. For uranyl, where V_{CF} is fourfold, this is true for the states $^3\Delta_{2g}$ and $^1\Delta_{2g}$. From Table 9 we see that these states (third and last states in the table) have large splittings; both of them have $\Omega = 2$. The other state with $\Omega = 2$ (fifth state in the table) can mix with these states and has a large crystal field splitting as well.

One of the questions with regard to the electronic spectrum of uranyl in the $Cs_2UO_2Cl_4$ crystal is at what energies the first excitations from Cl orbitals occur. We performed some very simple single-excitation CI calculations in order to answer this question. In these calculations the first excitations with substantial chlorine character start at approximately 33 000 cm^{-1}.

3.2. NpO_2^{2+}. The ground state of the free neptunyl ion has been discussed previously.[90] It has $\Omega = 5/2$ and is a combination of $^2\Delta_{5/2u}$ and $^2\Phi_{5/2u}$ $\Lambda-S$ components. In the absence of spin−orbit coupling, the $^2\Delta_u$ state is lower than the $^2\Phi_u$ state. Spin−orbit coupling splits the $^2\Phi_u$ state more than the $^2\Delta_u$, and the result is that the lower component of $^2\Phi_u$ becomes the dominant component of the ground state. In C_{2h} symmetry both the δ_u and ϕ_u orbitals split as shown in Table 1, but in D_{4h} only the δ_u orbitals split. Since the symmetry is close to D_{4h} the δ_u orbitals split more than the ϕ_u orbitals. From an SCF calculation the splitting for the δ_u orbitals is ca. 800 cm^{-1} and the splitting for the ϕ_u orbitals is ca. 200 cm^{-1}. Figure 3 shows the energy levels for these states at the SCF level of theory. After the crystal field splitting, the separation between the lower component of δ_u and the lower component of ϕ_u is larger than that for the free neptunyl ion. Another reason the separation is enlarged in the crystal is that the equatorial ligands will destabilize the ϕ_u orbitals more than the δ_u orbitals. Since the ϕ_u orbitals are localized in the equatorial plane while the δ_u orbitals have lobes above and below this plane, equatorial ligands have a more repulsive interaction with electrons in ϕ_u orbitals than with electrons in δ_u orbitals. This separation is important for the ground-state character.[90] When this separation is small the ϕ_u character dominates the ground state, but when it is large the δ_u character dominates. In the free neptunyl ion the first was true, but when it is doped into the $Cs_2UO_2Cl_4$ crystal the latter becomes true. At the SCF level in the crystal this separation is found to be ca. 5500 cm^{-1}. The corresponding separation for the free ion at the SCF level is 3000 cm^{-1}. As shown in Table 10, the ground state of neptunyl in the crystal is 86% δ_u. This is consistent with earlier EPR experiments,[99] which give different g factors for NpO_2^{2+} in $Cs_2UO_2Cl_4$ and $CsUO_2(NO_3)_3$.

Although the crystal environment affects the character of the neptunyl ground state in a major way, its affect on the changes in the neptunyl equilibrium bond distances and symmetric-stretch vibrational frequencies is modest and similar to the changes for uranyl. This is shown in Table 11. R_e (Np−O) stretches by ca. 0.06 Å at the SCF level and 0.04 Å at the CI

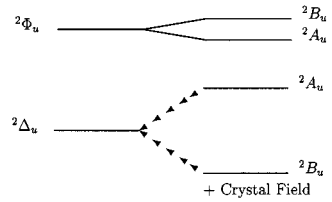

Figure 3. Splitting of the $^2\Delta_u$ and $^2\Phi_u$ states due to the crystal field.

TABLE 10: Wave Function Character for the Ground and Excited States of Neptunyl Doped into Crystalline $Cs_2UO_2Cl_4$

state	character
$1E_{1/2u}$	86% δ + 3% ϕ
$2E_{1/2u}$	40% δ + 49% ϕ
$3E_{1/2u}$	53% δ + 37% ϕ
$4E_{1/2u}$	89% ϕ
$5E_{1/2u}$	90% $\sigma\delta\phi$
$6E_{1/2u}$	84% π
$7E_{1/2u}$	68% $\sigma\delta^2$
$8E_{1/2u}$	83% π
$9E_{1/2u}$	88% $\sigma\delta\phi$
$10E_{1/2u}$	72% $\sigma\delta^2$
$11E_{1/2u}$	92% $\sigma\delta\phi$
$12E_{1/2u}$	84% $\sigma\delta\phi$

TABLE 11: Np−O Bond Distance and Symmetric-stretch Vibrational Frequency for the Ground State of Neptunyl Ion as a Free Ion and Embedded in the $Cs_2UO_2Cl_4$ Crystal

system (method)	R_e, Å	ν_1, cm^{-1}
free ion (SCF)	1.63	1146
free ion (CI)	1.66	1059
crystal (SCF)	1.69	920
crystal (CI)	1.70	950
crystal (exptl)	1.75[a]	802[b]

[a] From Makhyoun[89] (estimated). [b] From Denning et al.[83]

TABLE 12: Ground-State Tetrachloroneptunyl SCF Mulliken Population Analysis at R_e(Np−O) = 1.69 Å

	gross atomic populations					
atom	s	p	d	f	g	total
Np	2.218	5.633	1.721	3.434	0.004	13.011
O	3.840	9.027	0.046			12.914
Cl	7.914	23.140	0.021			31.075

TABLE 13: Np−O Bond Distances, R_e, for All the f^1 States and the First Charge-Transfer State of the Neptunyl Ion Doped into Crystalline $Cs_2UO_2Cl_4$

state	character	R_e, Å
$1E_{1/2u}$	86% δ + 3% ϕ	1.70
$2E_{1/2u}$	40% δ + 49% ϕ	1.72
$3E_{1/2u}$	53% δ + 37% ϕ	1.72
$4E_{1/2u}$	89% ϕ	1.72
$6E_{1/2u}$	84% π	1.75
$8E_{1/2u}$	83% π	1.75
$5E_{1/2u}$	90% $\sigma\delta\phi$	1.78

level and ν_1 decreases 226 cm^{-1} at the SCF level and 109 cm^{-1} at the CI level. As was mentioned in connection with the uranyl ion, the SCF comparisons are more informative about the crystal effect because the CI calculations for the free ion and the crystal are not completely equivalent. The CI calculations were performed only for the ground state, had 15 electrons correlated, and were equivalent to the ones for uranyl in the crystal.

The Mulliken population analysis for neptunyl in the crystal is shown in Table 12 at R_e(Np−O) = 1.69 Å. It is taken from an average SCF for the $^2\Delta$ and $^2\Phi$ states. The charge on Np is +1.989 as opposed to +2.345 for the free neptunyl ion and +2.078 for U in the crystal. The charge on each O is −0.457 and on each Cl is −0.769.

The neptunyl excited states are of two types: f → f where an electron in an f spin−orbital has been excited to another f spin−orbital, and charge-transfer where an electron in a bonding orbital has been excited to a nonbonding f orbital. According to these definitions, all the transitions in uranyl are of charge-transfer type. The name "charge-transfer" means that there is transfer of an electron (charge) from an oxygen orbital to an actinide orbital. The $3\sigma_u$ orbital, however, from which the excitations occur, is not a pure oxygen orbital. It is a mixture of both oxygen and actinide character with considerable bonding character, and the actinide character is larger than the oxygen character, approximately 70−30%. Thus the traditional nomenclature exaggerates the charge shift. Table 13 shows the R_e(Np−O) distances for some of the excited states of neptunyl in the crystal. The first four states each have a single electron in a nonbonding Np f orbital and have similar bond distances. The fπ orbitals, however, mix with the oxygen orbitals in an antibonding way and the states arising from occupation of these orbitals are higher in energy and have larger bond distances, indicating a weaker Np−O bond. The last state in the table is the first charge-transfer state and the bond distance is even longer since the bond is even further weakened. The results for the free neptunyl ion were very similar.[90] The calculations in this table, as well as the calculations in Table 14, to be discussed later, are multireference CI calculations with only seven electrons correlated. The correlation included in the calculations of excited states of neptunyl was less than that included for uranyl, for the reasons discussed in the methodology section.

Unlike the uranyl excited states, the neptunyl states are not split by the crystal field. In the linear ion they are Kramers doublets, so they cannot split further. All of them transform as the same irreducible representation in C_{2h}, $E_{1/2u}$. The adiabatic excitation energies are shown in Table 14. The first column

TABLE 14: Adiabatic Excitation Energies (in cm^{-1}) for NpO_2^{2+} Doped into $Cs_2NpO_2Cl_4$ Crystal

state	$Cs_2NpO_2Cl_4$	$Cs_2NpO_2Cl_4$(exptl)[a]	NpO_2^{2+} [b]	NpO_2^{2+} [c]
$1E_{1/2u}$	0	0	0	0
$2E_{1/2u}$	1 663	1 000	573	447
$3E_{1/2u}$	5 775	6 880.4	5 092	5 515
$4E_{1/2u}$	8 463	7 990	6 221	6 565
$5E_{1/2u}$	18 236	13 264.9	17 992	12 622
$6E_{1/2u}$	18 367	17 241.4	24 012	25 844
$7E_{1/2u}$	20 150	15 406.4	21 156	15 668
$8E_{1/2u}$	20 575	20 080.8	26 983	28 909
$9E_{1/2u}$	20 839	15 683	20 593	15 418
$10E_{1/2u}$	21 115	16 799.8	22 145	16 664
$11E_{1/2u}$	23 912		26 559	18 676
$12E_{1/2u}$	26 862	19 375.2	26 948	21 580

[a] From Denning et al.[83,84] [b] Adiabatic transitions, seven electrons correlated. [c] Vertical transitions, 15 electrons correlated.

gives the double group symmetry for each state (same for all states), the second column gives the calculated transition energies, the third column gives the experimental transition energies from Denning et al.,[83,84] the fourth column gives the free neptunyl ion transition energies calculated at the same level as the crystal calculations, and the fifth column gives the free neptunyl ion transition energies.[90] Thus, column four has adiabatic transitions, as does column two, which gives the calculated crystal transition energies. Furthermore, seven electrons were correlated as was done for the crystal.

A disappointing observation is that for many of these transitions the free-ion calculations give better agreement with the experimental values. This can be attributed to the fact that the CI calculations for the free ion have more correlation than the crystal calculations. This becomes more obvious when looking at the calculations in the fourth column. Calculating excited states is a difficult task; one has to pay much attention to treating all states equally. The MO's must be balanced for all states and the references must include all the same states. Furthermore, the excitation energies seem to be very sensitive to correlation. Comparing the two columns for the free ion with different levels of correlation, we see that the charge-transfer states are much more sensitive to correlation than are the f states. This should be expected since in charge-transfer transitions the occupation of the f orbitals changes. To draw some conclusion as to what the effect of the crystal is on the transition energies we should compare the second column with the fourth column where the calculations are similar. The transitions between states in the (δ_u, ϕ_u) space for the free ion are lower than they are in the crystal, while the transitions to the π_u states are higher in the free ion than in the crystal. We said earlier that the δ_u orbitals in the crystal split more than the ϕ_u, that the ϕ_u orbitals are raised more than the δ_u orbitals, and that the ground state has more δ_u character. Thus the ground state in the crystal is stabilized compared to the other states with more ϕ_u character and this is why the transition energies in this manifold increase. It is not simple to draw any conclusion about the effect of the crystal on the charge-transfer transitions.

To eliminate as many parameters as possible we will compare some SCF results, as was done in the uranyl case; the results illustrate the effects of the crystal field, but do not include the extensive mixing effects of the spin−orbit interaction, so that comparisons with Table 14 are not easily made. Thus Table 15 contains SCF vertical transition energies calculated at the equilibrium Np−O SCF distance (1.63 Å for neptunyl and 1.69 Å for neptunyl doped in the crystal). The excitations in the (δ_u, ϕ_u) manifold agree with our discussion about the CI results; the lowering of the δ_u orbital increases the transition energies.

TABLE 15: SCF Transition Energies (in cm^{-1}) for NpO_2^{2+} and $Cs_2NpO_2Cl_4$

C_{2h}	$Cs_2NpO_2Cl_4$	NpO_2^{2+}	$D_{\infty h}$	config
^2B_u	0	0	$^2\Delta_u$	$\sigma_u^2\delta_u^1$
^2A_u	795			
^2A_u	5 963	3 531	$^2\Phi_u$	$\sigma_u^2\phi_u^1$
^2B_u	6 139			
^2A_u	19 575	25 798	$^2\Pi_u$	$\sigma_u^2\pi_u^1$
^2B_u	19 765			
^4A_u	13 541	14 427	^4H_u	$\sigma_u^1\delta_u^1\phi_u^1$
^4B_u	15 214			
^4A_u	14 048	16 996	$^4\Sigma_u^-$	$\sigma_u^1\delta_u^2$

Charge-transfer transitions to $\sigma_u^1\delta_u^1\phi_u^1$ states do not change much, but transitions to $\sigma_u^1\delta_u^2$ states shift to lower energies by about 3000 cm^{-1} in the crystal. This can be explained again by the lowering in energy of the δ_u orbitals with respect to the ϕ_u orbitals. Going from the ground state to $\sigma_u^1\delta_u^1\phi_u^1$, the occupation of the δ_u orbitals does not change. Going from the ground state to $\sigma_u^1\delta_u^2$, the occupation of the δ_u orbitals increases by one, and thus an energy lowering occurs. The largest effect of the crystal environment, though, is on the $^2\Pi_u$ state. The red-shift in the crystal is more than 6000 cm^{-1}. The π_u orbitals differ from the δ_u and ϕ_u orbitals in that they mix with the oxygen orbitals. It is because of this mixing that they are higher in energy than the δ_u and ϕ_u orbitals. It may be that the lengthened bond distance in the crystal reduces the antibonding mixing with the oxygen orbitals, lowering their energy compared to the free ion.

It is important to note that in the uranyl crystal the agreement between theory and experiment for the uranyl ion is much better than for the neptunyl ion. The difference in the calculation of the two spectra in the crystal was that more electrons were frozen in the neptunyl calculations. In particular the $2\sigma_u$, $1\pi_u$, and $3\sigma_g$ orbitals were frozen for neptunyl but not for uranyl. It appears that these electrons are important for calculating transition energies and should be included whenever possible. In our neptunyl calculations it was computationally impossible to include them. We only correlated the $2\pi_u$ and $3\sigma_u$ electrons, which are even more essential. Further proof of the importance of these electrons comes in comparing the two calculations for the free neptunyl ion in Table 14. Again the difference between them is whether the same orbitals are correlated or not. The improvement in the transition energies when these orbitals are correlated is impressive; some of them improve by more than 5000 cm^{-1}. For our uranyl transition energies (Table 7) there are again two different calculations of the free uranyl ion. The difference is whether the $1\sigma_g$, $2\sigma_g$, $1\sigma_u$, and $1\pi_g$ electrons are correlated. These electrons are much less important in calculating the transition energies; the differences do not exceed 1000 cm^{-1}.

4. Conclusions

Calculations of the electronic spectra of two actinyl ions have been carried out in a crystalline environment in order to facilitate comparisons with the available spectroscopic data. Calculated bond-length increases, vibrational-frequency decreases, excitation-energy shifts, energy-level splittings, and changes in wave function character are generally found to useful accuracy and consistent with orbital-based ideas. Describing the crystalline interactions and relativistic effects to the needed accuracy is found to be generally less difficult than describing electron correlation. An improved level of electron correlation would make comparisons more straightforward as well as more accurate.

Acknowledgment. We thank R. G. Denning, S. R. Brozell, and Z. Zhang for helpful discussions of this work. S.M. was supported by a Presidential Fellowship from The Ohio State University. This work was supported in part by Pacific Northwest National Laboratory (PNNL) through Contract 200210, U.S. Department of Energy, the Mathematical, Information, and Computational Science Division, High-Performance Computing and Communications Program of the Office of Computational and Technology Research and by Argonne National Laboratory through the Actinide Synchrotron Studies project. PNNL is operated by Battelle Memorial Institute under contract DE-AC06-76RLO 1830. We used computational facilities at The Ohio State University (largely provided by the PNNL grant).

References and Notes

(1) Silva, R. J.; Nitsche, H. *Radiochim. Acta* **1995**, *70/71*, 377−396.
(2) *Computational chemistry for nuclear waste characterization and processing: Relativistic quantum chemistry of actinides;* Harrison, R. J., Ed.; Technical report, U.S. Department of Energy, 1999; http://www.emsl.pnl.gov/auth/actinides/newpub/source.html#top.
(3) Jacoby, M. *Chem. Eng. News* **1999**, *77* (15), 44−47.
(4) Cornehl, H. H.; Heinemann, C.; Marçalo, J.; Pires de Matos, A.; Schwarz, H. *Angew. Chem., Int. Ed. Eng.* **1996**, *35*, 891−894.
(5) Tomasi, J.; Persico, M. *Chem. Rev.* **1994**, *94*, 2027−2094.
(6) Solvent Effects and Chemical Reactivity. In *Understanding Chemical Reactivity*; Tapia, O., Bertrán, J., Eds.; Kluwer: Dordrecht, The Netherlands, 1996; Vol. 17.
(7) Pisani, C.; Dovesi, R.; Roetti, C. Hartree−Fock Ab Initio Treatment of Crystalline Systems. In *Lecture Notes in Chemistry*: Springer: Berlin, 1988; Vol. 48.
(8) Fulde, P. Electron Correlations in Molecules and Solids. In *Solid-State Sciences*, 3rd ed.; Springer: Berlin, 1995; Vol. 100.
(9) Sugano, S.; Shulman, R. G. *Phys. Rev.* **1963**, *130*, 517−530.
(10) Ellis, D. E.; Freeman, A. J.; Ros, P. *Phys. Rev.* **1968**, *176*, 688−707.
(11) Wachters, A. J. H.; Nieuwpoort, W. C. *Phys. Rev. B* **1972**, *5*, 4291−4301.
(12) Almlöf, J.; Wahlgren, U. *Theor. Chim. Acta* **1973**, *28*, 161−168.
(13) Shashkin, S. Y.; Goddard III, W. A. *Phys. Rev. B* **1986**, *33*, 1353−1359.
(14) Ewald, P. P. *Ann. Phys.* **1921**, *64*, 253−287.
(15) Brown, R. D.; Burton, P. G. *Theor. Chim. Acta* **1970**, *18*, 309−328.
(16) Pueyo, L.; Richardson, J. W. *J. Chem. Phys.* **1977**, *67*, 3583−3591.
(17) Barandiarán, Z.; Pueyo, L.; Gómez Beltrán, J. *J. Chem. Phys.* **1983**, *78*, 4612−4618.
(18) Winter, N. W.; Pitzer, R. M. Theoretical methods for the study of transition metals in crystals. In *Tunable Solid State Lasers*; Hammerling, P., Budgor, A. B., Pinto, A., Eds.; Vol. 47 of *Springer Series in Optical Science*; Springer: Berlin, 1985; pp 164−171.
(19) Winter, N. W.; Pitzer, R. M.; Temple, D. K. *J. Chem. Phys.* **1987**, *86*, 3549−3556.
(20) Winter, N. W.; Pitzer, R. M.; Temple, D. K. *J. Chem. Phys.* **1987**, *87*, 2945−2953.
(21) Temple, D. K. Ab Initio Cluster Study of Crystalline NaF. Ph.D. Thesis, University of California, Davis, CA, 1992.
(22) Barandiarán, Z.; Seijo, L. *J. Chem. Phys.* **1988**, *89*, 5739−5745.
(23) Barandiarán, Z.; Seijo, L. Beyond the embedded-cluster approximation: an ab initio treatment of polarization effects. In *Cluster Models for Surface and Bulk Phenomena*; Bagus, P. S., Parmigiani, F., Eds.; Vol. 283 of *NATO ASI Series B: Physics*; Plenum: New York, 1992; pp 565−576.
(24) Whitten, J. L.; Pakkanen, T. A. *Phys. Rev. B* **1980**, *21*, 4357−4367.
(25) Whitten, J. L. *Phys. Rev. B* **1981**, *24*, 1810−1817.
(26) Kunz, A. B.; Vail, J. M. *Phys. Rev. B* **1988**, *38*, 1058−1063.
(27) Kantorovich, L. N. *J. Phys. C* **1988**, *21*, 5041−5056.
(28) Kantorovich, L. N. *J. Phys. C* **1988**, *21*, 5057−5073.
(29) Pisani, C.; Dovesi, R.; Nada, R.; Kantorovich, L. N. *J. Chem. Phys.* **1990**, *92*, 7448−7460.
(30) Shukla, A.; Dolg, M.; Stoll, H.; Fulde, P. *Chem. Phys. Lett.* **1996**, *262*, 213−218.
(31) Shukla, A.; Dolg, M.; Fulde, P.; Stoll, H. *Phys. Rev. B* **1998**, *57*, 1471−1483.
(32) Klaproth, M. H. *Chem. Ann.* **1789**, *2*, 387−403.
(33) Stokes, G. G. *Philos. Trans. R. Soc. London* **1852**, 463−562.
(34) Becquerel, H. *C. R. Hebd. Seances Acad. Sci.* **1896**, *122*, 420−421.

(35) Becquerel, E. *C. R. Hebd. Seances Acad. Sci.* **1872**, *75*, 296−303.
(36) Dieke, G. H.; Duncan, A. B. F. Spectroscopic properties of Uranium Compounds. In *National Nuclear Energy Series, Division III*; McGraw-Hill: New York, 1949; Vol. 2.
(37) Bell, J. T.; Biggers, R. E. *J. Mol. Spectrosc.* **1968**, *25*, 312−329.
(38) Rabinowitch, E.; Belford, R. L. *Spectroscopy and Photochemistry of Uranyl Compounds*; Pergamon: New York, 1964.
(39) Denning, R. G.; Snellgrove, T. R.; Woodwark, D. R. *Mol. Phys.* **1975**, *30*, 1819−1828.
(40) Denning, R. G.; Snellgrove, T. R.; Woodwark, D. R. *Mol. Phys.* **1976**, *32*, 419−442.
(41) Denning, R. G.; Snellgrove, T. R.; Woodwark, D. R. *Mol. Phys.* **1979**, *37*, 1089−1107.
(42) Barker, T. J.; Denning, R. G.; Thorne, R. G. *Inorg. Chem.* **1987**, *26*, 1721−1732.
(43) McGlynn, S. P.; Smith, J. K. *J. Mol. Spectrosc.* **1961**, *6*, 164−187.
(44) Görller-Walrand, C.; Vanquickenborne, L. G. *J. Chem. Phys.* **1972**, *57*, 1436−1440.
(45) Eisenstein, J. C.; Pryce, M. H. L. *Proc. R. Soc. London* **1955**, *A229*, 20−38.
(46) Jørgensen, C. K. *Acta Chem. Scand.* **1957**, *11*, 166−178.
(47) Denning, R. G.; Snellgrove, T. R.; Woodwark, D. R. *Mol. Phys.* **1979**, *37*, 1109−1143.
(48) Boring, M.; Wood, J. H.; Moskowitz, J. W. *J. Chem. Phys.* **1975**, *63*, 638−642.
(49) Ellis, D. E.; Rosén, A.; Walch, P. F. *Int. J. Quantum Chem., Symp.* **1975**, *9*, 351−358.
(50) Walch, P. F.; Ellis, D. E. *J. Chem. Phys.* **1976**, *65*, 2387−2392.
(51) Yang, C. Y.; Johnson, K. H.; Horsley, J. A. *J. Chem. Phys.* **1978**, *68*, 1001−1005.
(52) Boring, M.; Wood, J. H. *J. Chem. Phys.* **1979**, *71*, 392−399.
(53) Tatsumi, K.; Hoffmann, R. *Inorg. Chem.* **1980**, *19*, 2656−2658.
(54) Wood, J. H.; Boring, M.; Woodruff, S. B. *J. Chem. Phys.* **1981**, *74*, 5225−5233.
(55) Wadt, W. R. *J. Am. Chem. Soc.* **1981**, *103*, 6053−6057.
(56) DeKock, R. L.; Baerends, E. J.; Boerrigter, P. M.; Snijders, J. G. *Chem. Phys. Lett.* **1984**, *105*, 308−316.
(57) Pyykkö, P.; Laaksonen, L. *J. Phys. Chem.* **1984**, *88*, 4892−4895.
(58) Pyykkö, P.; Laakkonen, L. J.; Tatsumi, K. *Inorg. Chem.* **1989**, *28*, 1801−1805.
(59) Pyykkö, P.; Lohr, L. L., Jr. *Inorg. Chem.* **1981**, *20*, 1950−1959.
(60) Pyykkö, P.; Li, J.; Runeberg, N. *J. Phys. Chem.* **1994**, *98*, 4809−4813.
(61) Pershina, V. G.; Ionova, G. V.; Suraeva, N. I. *Russian J. Inorg. Chem.* **1990**, *35*, 1178−1181.
(62) Ionova, G. V.; Pershina, V. G.; Suraeva, N. I. *Russian J. Inorg. Chem.* **1991**, *36*, 175−177.
(63) Craw, J. S.; Vincent, M. A.; Hillier, I. H. *J. Phys. Chem.* **1995**, *99*, 10181−10185.
(64) Wahlgren, U.; Schimmelpfennig, B.; Jusuf, S.; Stromsnes, H.; Gropen, O.; Maron, L. *Chem. Phys. Lett.* **1998**, *287*, 525−530.
(65) de Jong, W. A.; Visscher, L.; Nieuwpoort, W. C. *J. Mol. Struct.* **1999**, *458*, 41−52.
(66) Schreckenbach, G.; Hay, P. J.; Martin, R. L. *Inorg. Chem.* **1998**, *37*, 4442−4451.
(67) Schreckenbach, G.; Hay, P. J.; Martin, R. L. *J. Comput. Chem.* **1999**, *20*, 70−90.
(68) Hay, P. J.; Martin, R. L.; Schreckenbach, G. *J. Phys. Chem. A* **2000**, *104*, 6259−6270.
(69) Ismail, N.; Heully, J.; Saue, T.; Daudey, J.; Marsden, C. J. *Chem. Phys. Lett.* **1999**, *300*, 296−302.
(70) Dyall, K. G. *Mol. Phys.* **1999**, *96*, 511−518.
(71) Zhang, Z.; Pitzer, R. M. *J. Phys. Chem. A* **1999**, *103*, 6880−6886.
(72) Zhang, Z.; Harrison, R. J.; Pitzer, R. M. Ab initio study of uranyl complexation by various anions in solutions. In *Book of Abstracts*, 217th ACS National Meeting, Anaheim, CA; American Chemical Society: Washington, DC, 1999; NUCL-091.
(73) Nichols, J. A.; Windus, T.; Dixon, D. A. Density functional theory of actinide complexes. In *Book of Abstracts*, 217th ACS National Meeting, Anaheim, CA; American Chemical Society: Washington, DC, 1999; NUCL-095.
(74) Nichols, E. L.; Howes, H. L. *Fluorescence of the Uranyl Salts;* Carnegie Institute of Washington, 1919.
(75) Jørgensen, C. K.; Reisfeld, R. *Struct. Bonding (Berlin)* **1982**, *50*, 121−171.
(76) Denning, R. G. *Struct. Bonding (Berlin)* **1992**, *79*, 215−276.
(77) Sjoblom, R.; Hindman, J. C. *J. Am. Chem. Soc.* **1951**, *73*, 1744−1751.
(78) Waggener, W. C. *J. Phys. Chem.* **1958**, *62*, 382−383.
(79) Hagan, P. G.; Cleveland, J. M. *J. Inorg. Nucl. Chem.* **1966**, *28*, 2905−2909.
(80) Carnall, W. T. Absorption and luminescence spectra. In *Gmelin Handbooks of Inorganic Chemistry, Transuranium Elements A2*, 8th ed.; Verlag Chemie GMBH: Weinheim/Bergstrasse, 1973; Chapter 8.2, pp 49−80.
(81) Stafsudd, O. M.; Leung, A. F.; Wong, E. Y. *Phys. Rev.* **1969**, *180*, 339−343.
(82) Leung, A. F.; Wong, E. Y. *Phys. Rev.* **1969**, *187*, 504−511.
(83) Denning, R. G.; Norris, J. O. W.; Brown, D. *Mol. Phys.* **1982**, *46*, 287−323.
(84) Denning, R. G.; Norris, J. O. W.; Brown, D. *Mol. Phys.* **1982**, *46*, 325−364.
(85) Eisenstein, J. C.; Pryce, M. H. L. *J. Res. Natl. Bur. Stand. A*, **1965**, *69*, 217−235.
(86) Ionova, G. V.; Pershina, V. G.; Suraeva, N. I. *Sov. Radiochem.* **1989**, *31*, 9−14.
(87) Ionova, G. V.; Pershina, V. G.; Suraeva, N. I. *Sov. Radiochem.* **1990**, *31*, 379−385.
(88) Pershina, V. G.; Ionova, G. V.; Suraeva, N. I. *Sov. Radiochem.* **1990**, *31*, 386−391.
(89) Makhyoun, M. A. *Inorg. Chem.* **1987**, *26*, 3592−3595.
(90) Matsika, S.; Pitzer, R. M. *J. Phys. Chem. A* **2000**, *104*, 4064−4068.
(91) Slater, J. C. *Adv. Quantum Chem.* **1972**, *6*, 1−92.
(92) Hall, D.; Rae, A. D.; Waters, T. N. *Acta Crystallogr.* **1966**, *20*, 160−162.
(93) Watkin, D. J.; Denning, R. G.; Prout, K. *Acta Crystallogr.* **1991**, *C47*, 2517−2519.
(94) von Szentpály, L.; Fuentealba, P.; Preuss, H.; Stoll, H. *Chem. Phys. Lett.* **1982**, *93*, 555−559.
(95) Christiansen, P. A.; Ermler, W. C.; Pitzer, K. S. *Annu. Rev. Phys. Chem.* **1985**, *36*, 407−432.
(96) Blaudeau, J. P.; Brozell, S. R.; Matsika, S.; Zhang, Z.; Pitzer, R. M. *Int. J. Quantum Chem.* **2000**, *77*, 516−520.
(97) Dunning, Jr, T. H. *J. Chem. Phys.* **1989**, *90*, 1007−1023.
(98) Yabushita, S.; Zhang, Z.; Pitzer, R. M. *J. Phys. Chem. A* **1999**, *103*, 5791−5800.
(99) Leung, A. F.; Wong, E. Y. *Phys. Rev.* **1969**, *180*, 380−385.